

LASER INTERFEROMETER GRAVITATIONAL WAVE OBSERVATORY
-LIGO-
CALIFORNIA INSTITUTE OF TECHNOLOGY
MASSACHUSETTS INSTITUTE OF TECHNOLOGY
COLUMBIA UNIVERSITY IN THE CITY OF NEW YORK

Technical Note LIGO-T1700039

Wednesday, July 19, 2017

**Timing Witness Signals Indicate Trustworthy Timing
for G268556, a BBH Event Candidate**

Stefan Countryman, Zsuzsa Márka
Columbia University

This is a working note
of the LIGO Project

California Institute of Technology
LIGO Project – MS 51-33
Pasadena CA 91125
Phone (626) 395-2129
Fax (626) 304-9834
E-mail: info@ligo.caltech.edu

Massachusetts Institute of Technology
LIGO Project, MIT NW22-295,
185 Albany St., Cambridge, MA 02139 USA
Phone (617) 253 4824
Fax (617) 253 7014
E-mail: info@ligo.mit.edu

Columbia University
Columbia Astrophysics Laboratory
Pupin Hall - MS 5247
New York NY 10027
Phone (212) 854-8209
Fax (212) 854-8121
E-mail: geco.cu@gmail.com

WWW: <http://markalab.org/> <http://www.ligo.caltech.edu>



Synopsis

*Advanced LIGO data is taken by a DAQ that is directly driven in hardware by the Advanced LIGO Timing **Distribution** System that ensures end-to-end hardware-based timing signal integrity between the received GPS signal and the ADC boards. The Advanced LIGO Timing **Diagnostic** System is a separate additional hardware that provides additional layers of timing information and crosschecks to enable us to have versatile diagnostic information.*

As an extra precaution, we examined the timing witness signals to ensure that the aLIGO datastream's timing was perfect around Event Candidate G268556, also referred to as GW170104, observed at 1167559936= Wed Jan 04 10:11:58 UTC 2017. We found that the DuoTone witness indicated excellent timing performance on the sub-microsecond level and the IRIG-B signals indicated precise second decoding.

1. Introduction

The advanced LIGO timing system is implemented in hardware. Each and every board in the chain was tested multiple times in different environments, including end-to-end test using long fibers - it performs for tens of ns and the GPS is rated for few hundred ns. This is the primary performance measure of the well-working timing system that is below 1 μ s.

Additionally, independent hardware generated GPS synchronized timing witness channels are recorded along with the aLIGO datastream: the DuoTone and the IRIG-B datastreams at each end-stations. The phase of the DuoTone signals allows sub-microsecond accuracy determination of the datastream's shift from the perfect agreement with the GPS time. Since the DuoTone signal is repeated in every second, it is prudent to also look at the IRIG-B signal that has a phase allowing time verification on the ms level and a full timecode allowing the determination of absolute YEAR:MONTH:DAY-HOUR:MINUTE:SECOND. Therefore the DuoTone and IRIG-B signals together cover all possible timeshifts, and the most feared small shifts redundantly.

In this document we provide visual proof that the phase of the witness signals did not move from the nominal value even for a second during the hour surrounding the GW170104 event.

2. DuoTone Signal Measurements

Each aLIGO ADC chassis contain a timing Slave board with a DuoTone daughterboard installed. The Slave-DuoTone assembly pairs provide the precise pulses that allow the ADC to record the aLIGO data at 65536Hz rate; the phase of this low phase noise ADC clock is synchronized to the GPS 1PPS rising edge. Besides this mission critical functionality, each DuoTone board provide a so called DuoTone diagnostic signal(**Y**):

$$Y1 = A * \sin(2 * \pi * 960 * (T + \Delta T));$$

$$Y2 = A * \sin(2 * \pi * 961 * (T + \Delta T));$$

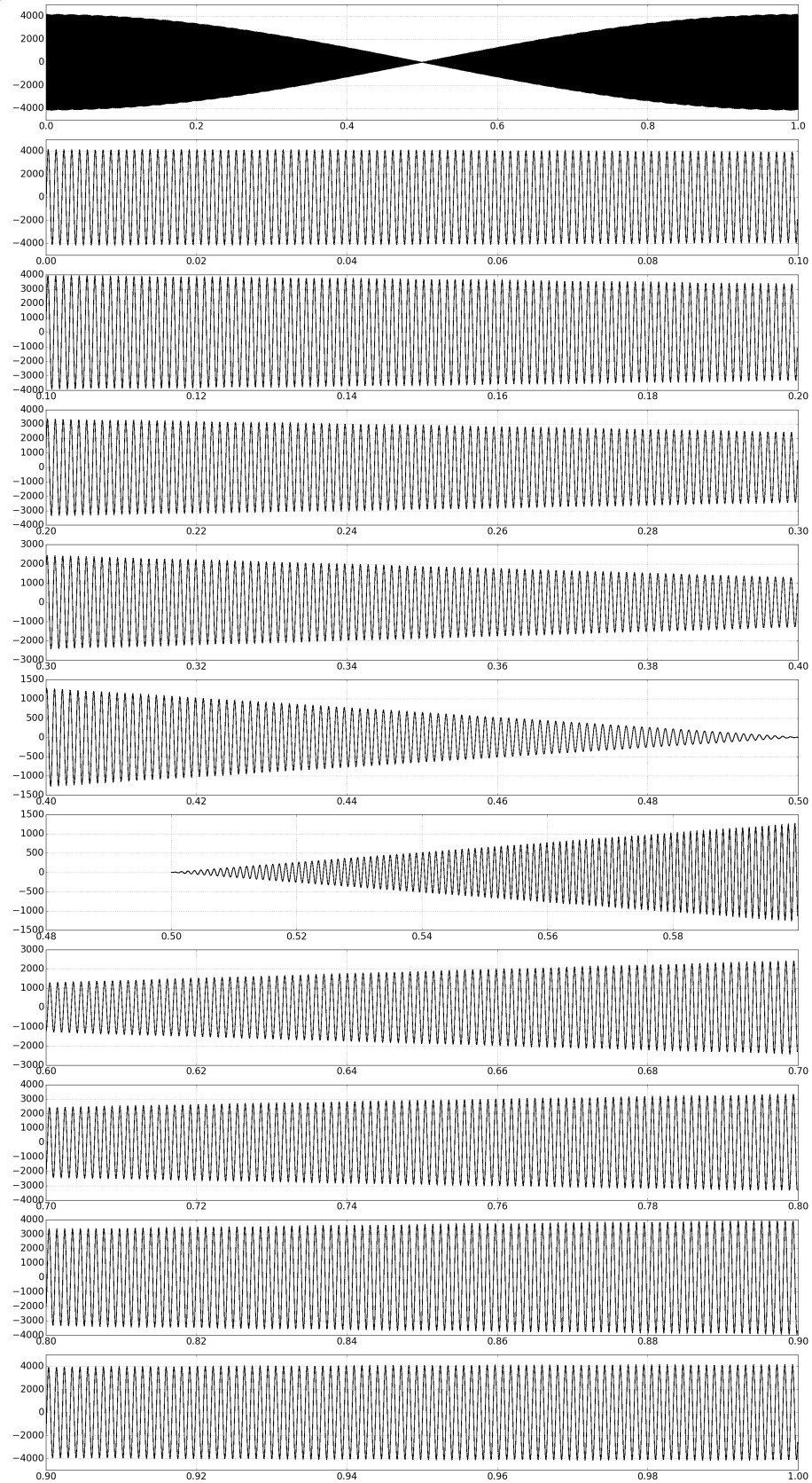
$$Y = Y1 + Y2 + \Delta A;$$

960Hz is chosen as it is a harmonic of 60Hz, to further preserve GW signal frequency space. The identical individual amplitude A is nominally 2.5V centered around $\Delta A = 0V$ and ΔT describes the position of the GPS 1PPS rising edge compared to the 0° common phase of the generated DuoTone, which we call the ‘coincident zero crossing’ (the time where the phase of both sinusoidal components becomes zero). The coincident zero crossing clearly and unambiguously repeats once in every second. The sinusoids produced by the slave-duotone timing stack (see e.g. [LIGO-E0900019](#)) are thus hardware synchronized to the GPS time in every second with a well-characterized delay of ΔT for the zero crossing (see [LIGO-T1500513](#)), and therefore even order of \sim microsecond deviations in timing performance would result in alteration of duotone signal shape and change in zero crossing time.

We checked for deviations in duotone signal shape by ‘stacking’ 1 second long consecutive segments of duotone signals (i.e. plotting each 1 second long segments on top of each other). The data covered two half-an-hour long time intervals closest to the event candidate time. On figures 1-4, each consecutive second of the measured DuoTone signal was plotted and *stacked* on top of each other for a 30 minutes long data window. The x axis represents one second duration of DuoTone segments. Since the DuoTone repeats its waveform every second, ideally all DuoTone curves on the plot are identical to each other, and they should look like a single curve on the plot even though the plot has $30 \times 60 = 1800$ curves plotted on top of each other. If there are seconds where the timing of the DuoTone signals are shifted from the nominal value, or where the signal suffered some sort of degradation, noise, or glitching, the *stacked* signal’s curve would no longer resemble a single waveform, lose fidelity and the deviation from normal would be clearly visible to the human eye. In the next 4 pages (figures 1-4) we show the *stacked* curves for the X-end-stations of the LLO and LHO aLIGO observatories. There are no visible deviations from the normal—as intended, the signal is periodic to a high degree of accuracy, giving the *stacked* plots the appearance of a single second of DuoTone signal.



Figure 1
Overlay of DuoTone, Hanford EX
Jan 04, 2017 9:41:58 to Jan 04, 2017 10:11:57





Overlay of DuoTone, Hanford EX
Jan 04, 2017 10:11:58 to Jan 04, 2017 10:41:58

Figure 2

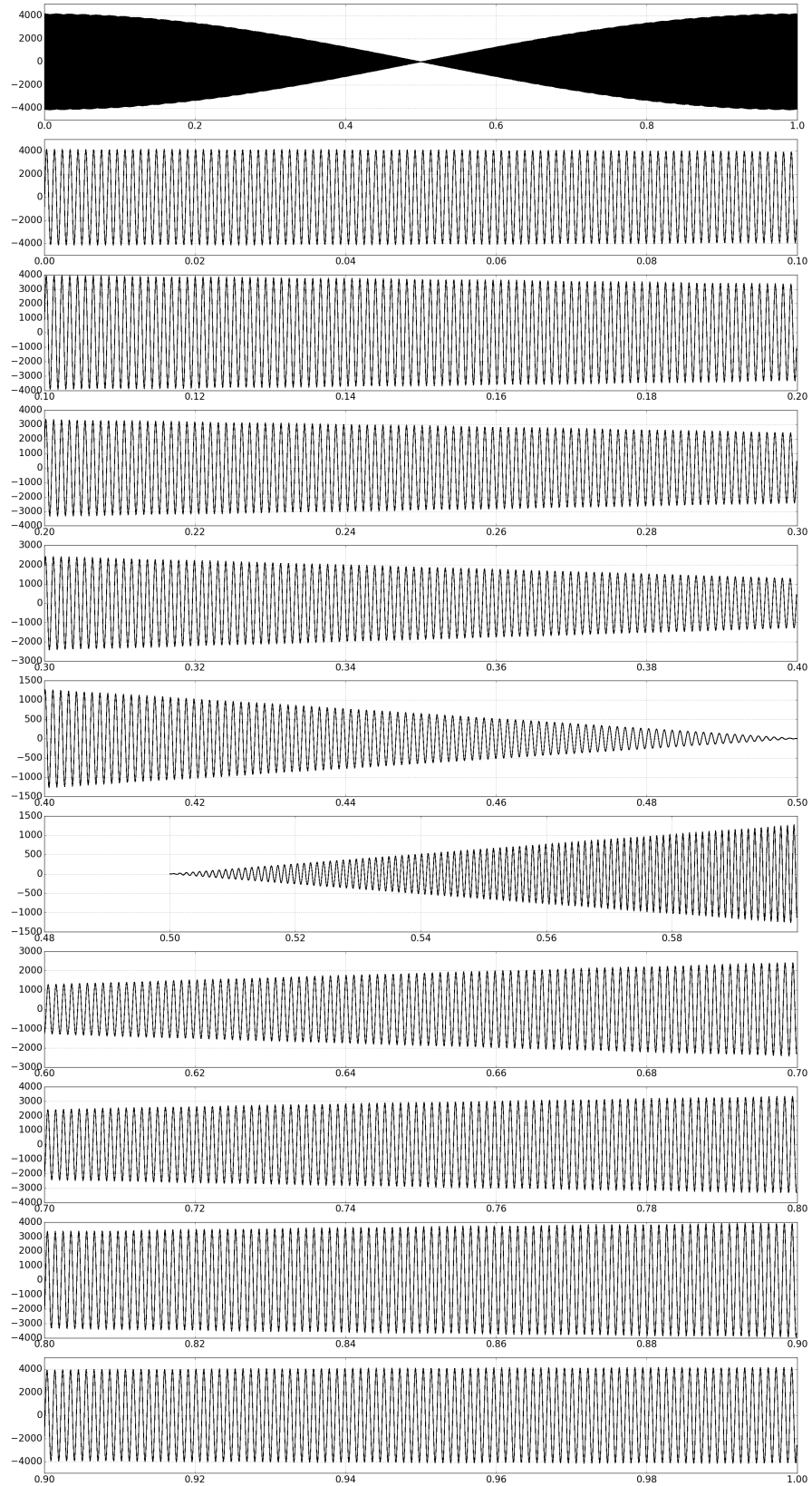


Figure 3

Overlay of DuoTone, Livingston EX
Jan 04, 2017 9:41:58 to Jan 04, 2017 10:11:57

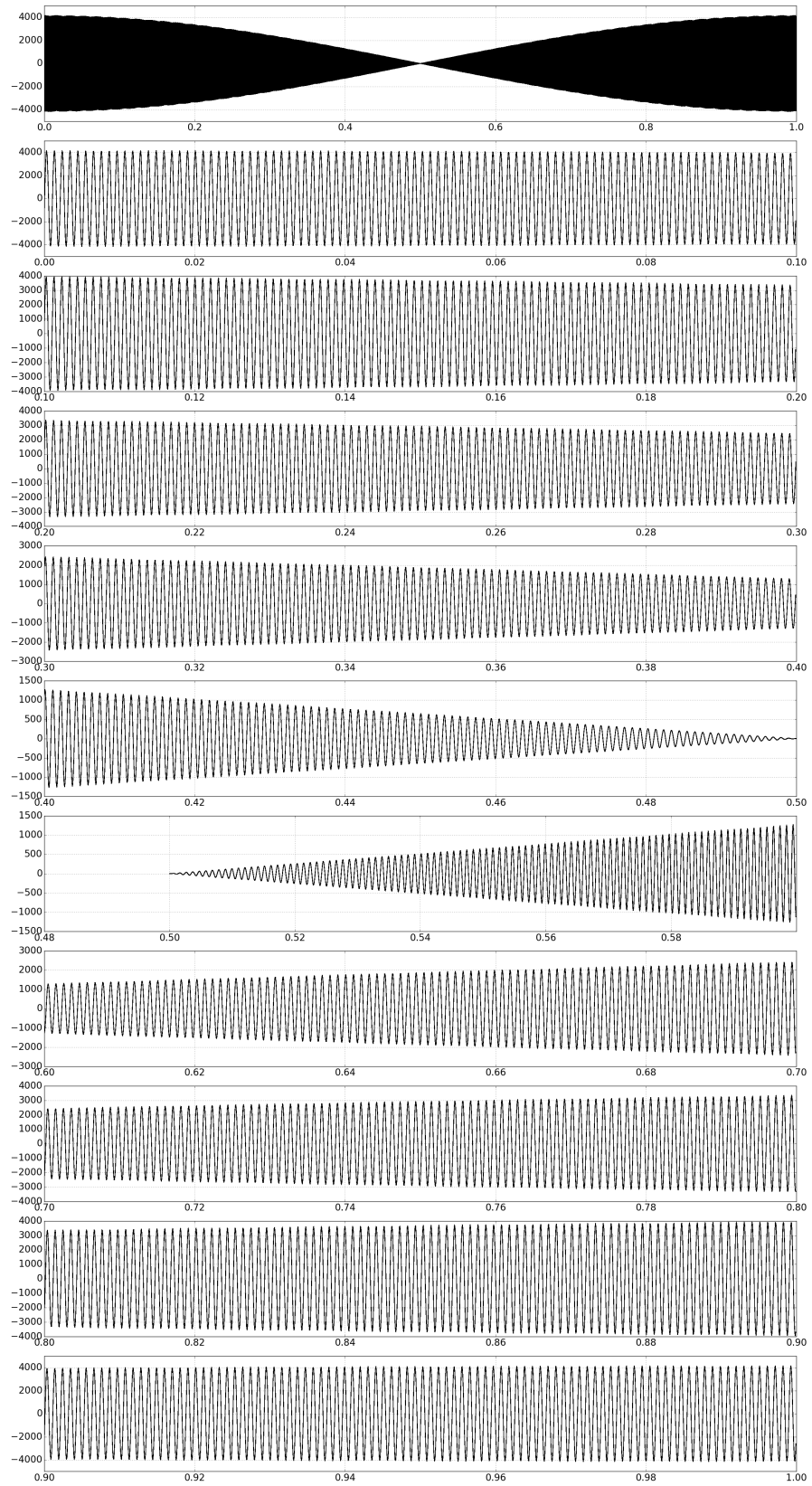
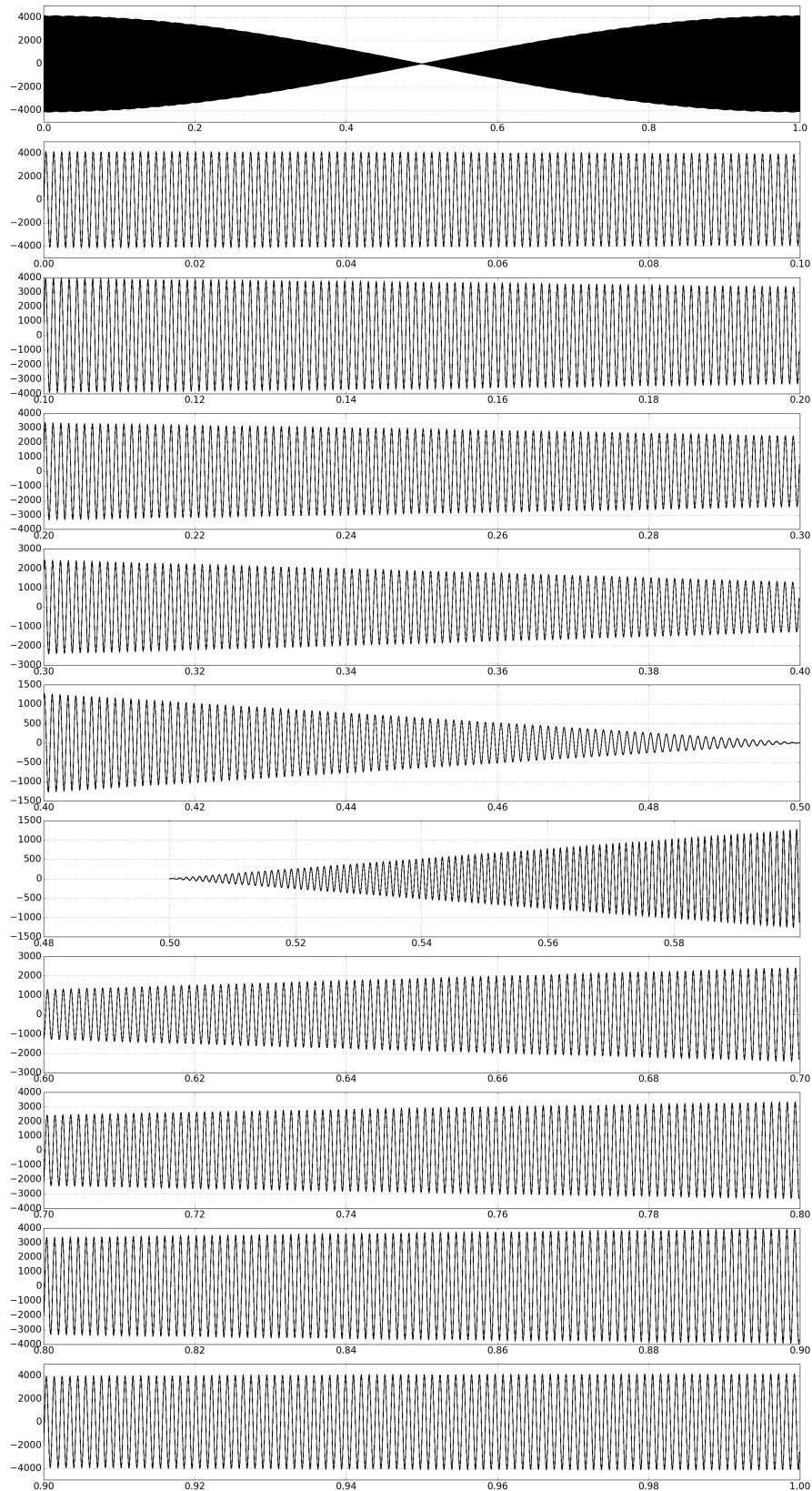


Figure 4

Overlay of DuoTone, Livingston EX
Jan 04, 2017 10:11:58 to Jan 04, 2017 10:41:58





3. DuoTone Signal Phase

Beyond *stacking* 1 second long segments of duotone signals on top of each other (see section 2), we also averaged the one second long waveforms and plotted the averaged DuoTone signal to verify the agreement and errors to higher accuracy.

The following 6 pages (figures 5-10) show the zero crossing region of the second-to-second average of the DuoTone witness signals around the second edge, zoomed-in at different magnifications in the x-axis. When the DuoTone signals are symmetric around the 0V level, the zero crossing should be delayed compared to the second tic of the datastream by $\sim 50.25\mu\text{s}$ ($6.70\mu\text{s}$ of this is due to an inherent delay on the timing Slave-DuoTone stack (see [LIGO-T1500513](#)), and the rest is due to 65536Hz to 16384Hz decimation filter. See [T1700024](#) document for characterization of DuoTone timing witness channels for O2.

On the figures the open circles reflect the average signal, the green error bars indicate the standard deviation, and the ends of the fine black error bars show the maximum/minimum for each data point. The line through the data points guide the eye to help visualize the zero crossing, which is most visible at the medium timescale plotted, and is at around $50.7\mu\text{s}$. The plots indicate precise agreement with the expected place of the zero crossing and confirm the independent verification measurement by LHO and LLO rapid response team (see [EVNT log](#)).

The purpose of this study was not the measurement of the already known DuoTone delay, but to verify the stable microsecond-level performance of the timing system at around the time of the candidate event. The DuoTone witness signals indeed indicate *very small errors*: The highest magnification of a representative data point (the last plot of three for each detector) shows in green the standard deviation of measurements for the point closest to the zero crossing for the hour surrounding the GW170104 event candidate and the error bars indicate the observed maximum and minimum.

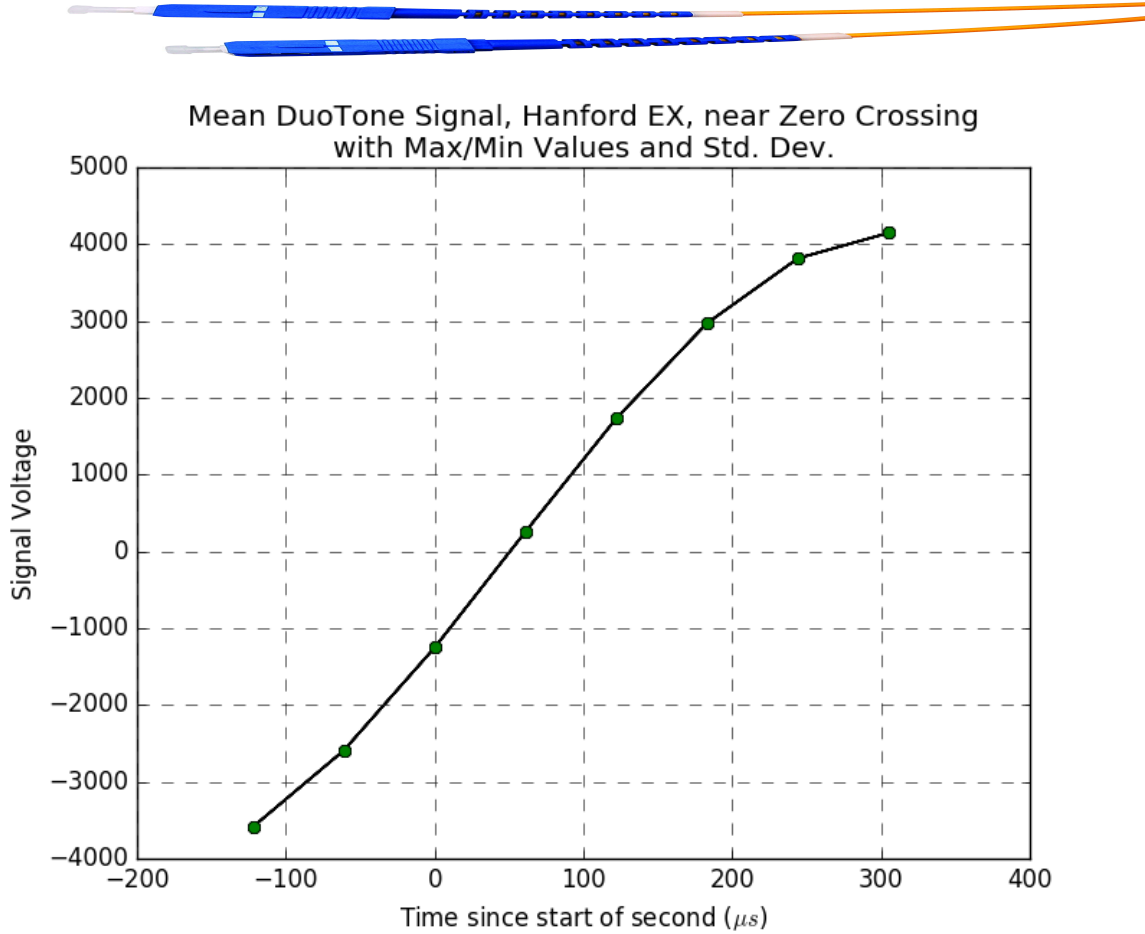


Figure 5: Zero crossing region of the second-to-second average of the DuoTone witness signals around the second edge at Hanford EX for the hour surrounding the GW170104 event candidate. The line through the data points guide the eye to help visualize the zero crossing. Please note that the errors on each point are so small that they are covered by the circular symbol.

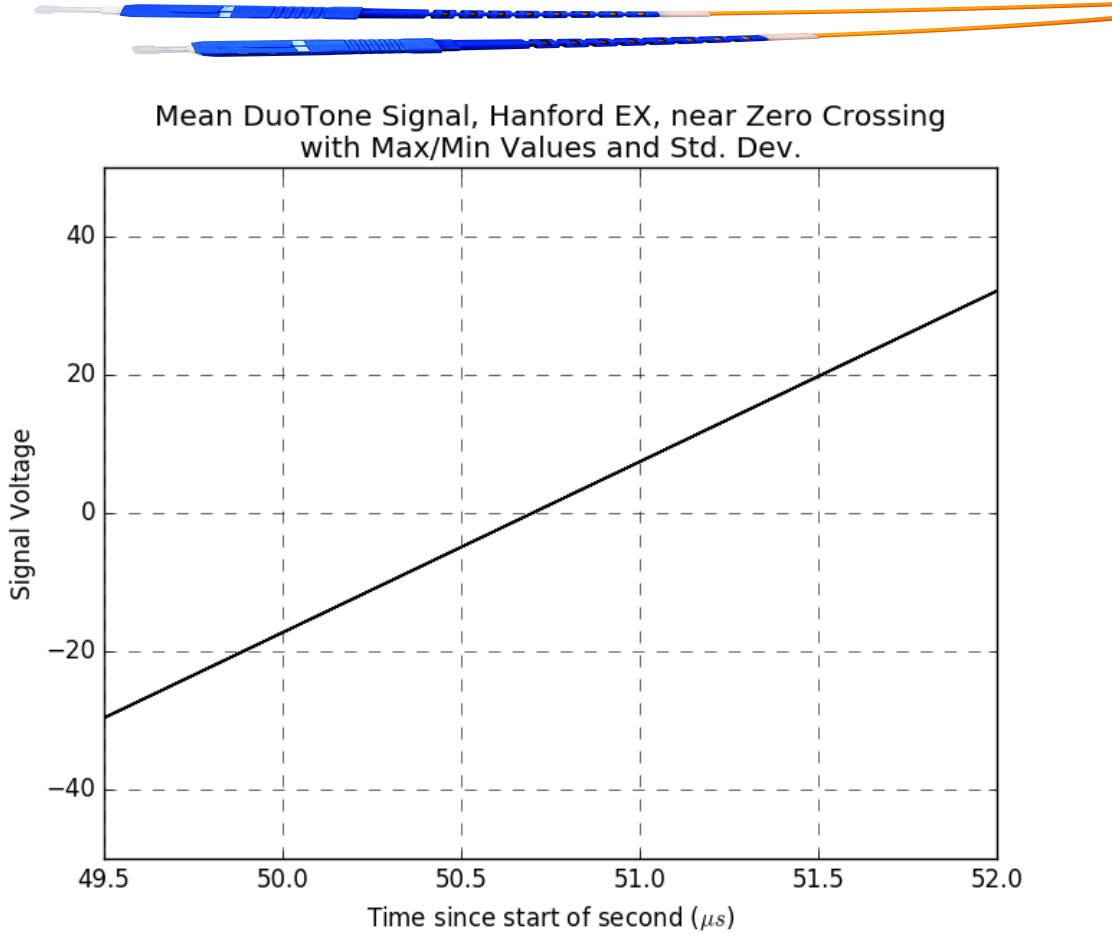


Figure 6: Zero crossing region of the second-to-second average of the DuoTone witness signals around the second edge at Hanford EX for the hour surrounding the GW170104 event candidate. Open circle reflect the average signal, the green error bars indicate the standard deviation, and the ends of the fine black error bars show the maximum/minimum for each data point. Please note that the green error bar is so small that it is still covered by the circular symbol. The line through the data points guide the eye to help visualize the zero crossing which is best visible on this magnification setting and is at $\sim 50.7\mu\text{s}$, out of which $50.25\mu\text{s} = 6.70\mu\text{s}$ (DuoTone generation delay) + $43.55\mu\text{s}$ (decimation filter delay) is accounted for.

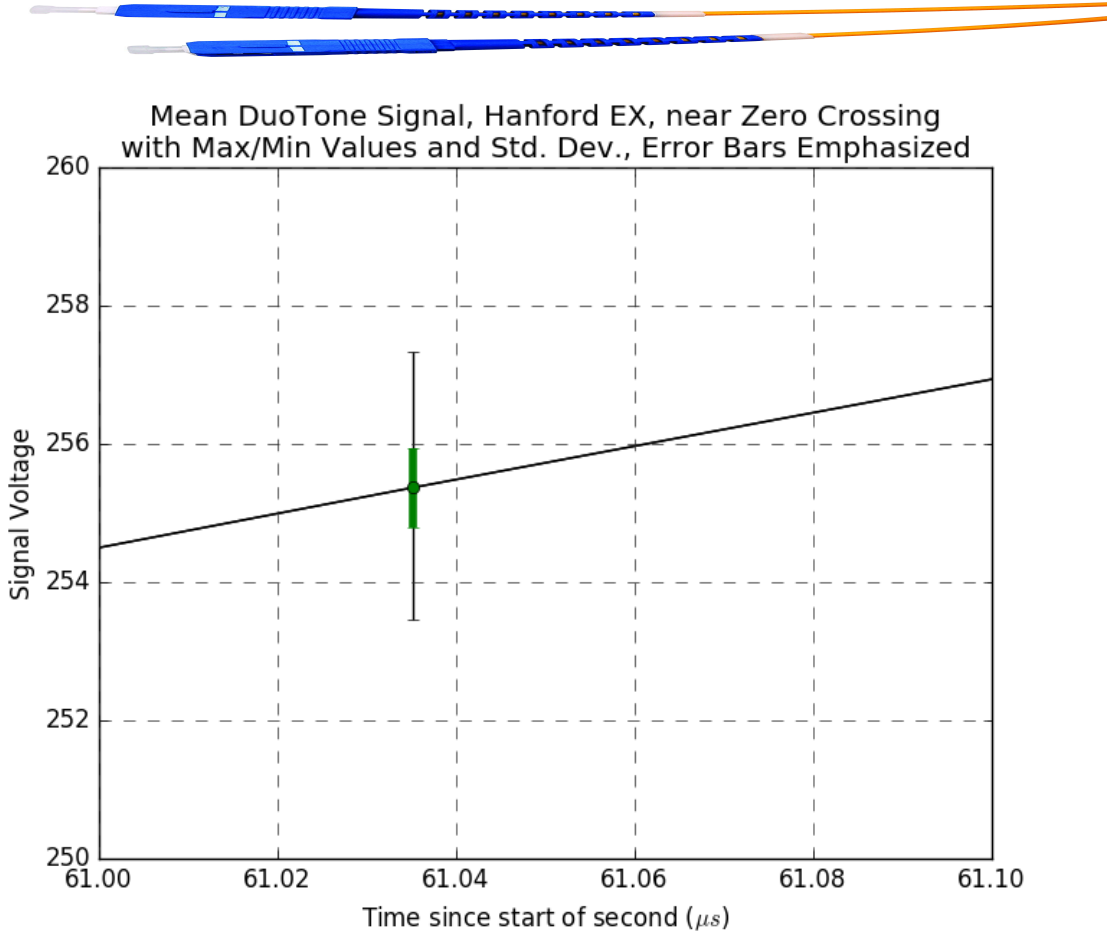


Figure 7: Zero crossing region of the second-to-second average of the DuoTone witness signals around the second edge at Hanford EX for the hour surrounding the GW170104 event candidate. The open circle reflect the average signal, the green error bar indicates the standard deviation, and the ends of the fine black error bar shows the maximum/minimum for the data point. The size of the green error bar indicates very small error on the zero crossing.

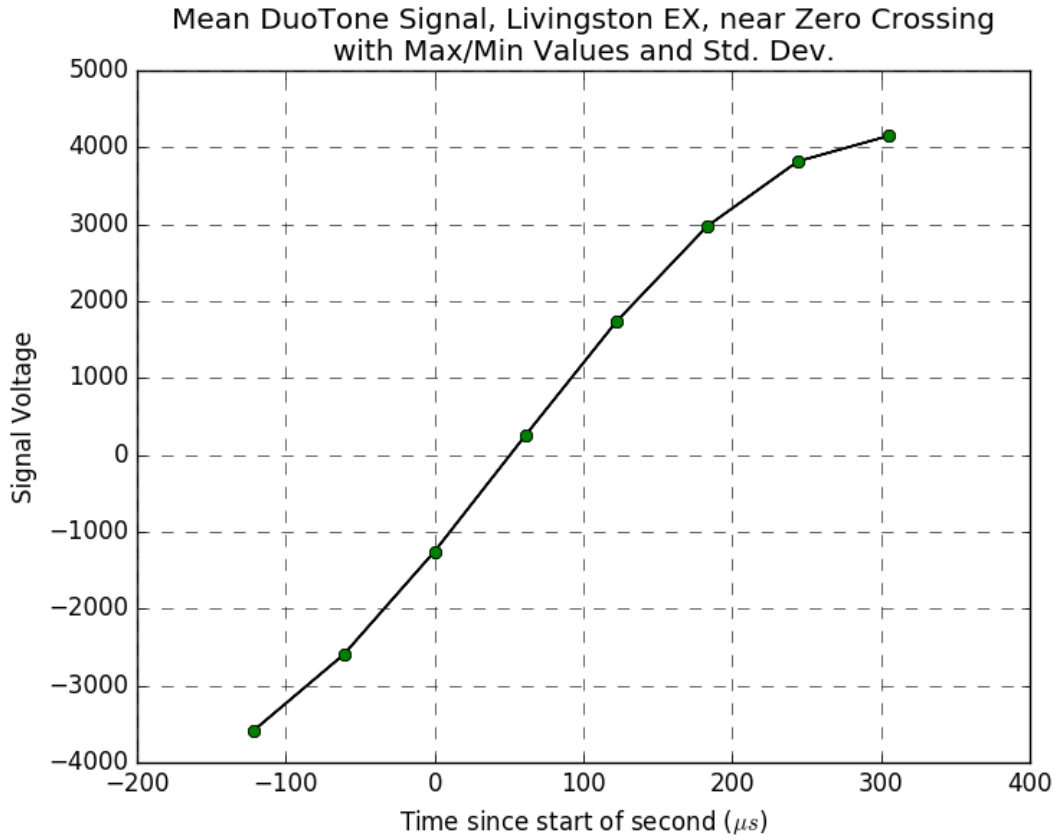


Figure 8: Zero crossing region of the second-to-second average of the DuoTone witness signals around the second edge at Livingston EX for the hour surrounding the GW170104 event candidate. The line through the data points guide the eye to help visualize the zero crossing. Please note that the errors on each point are so small that they are covered by the circular symbol.

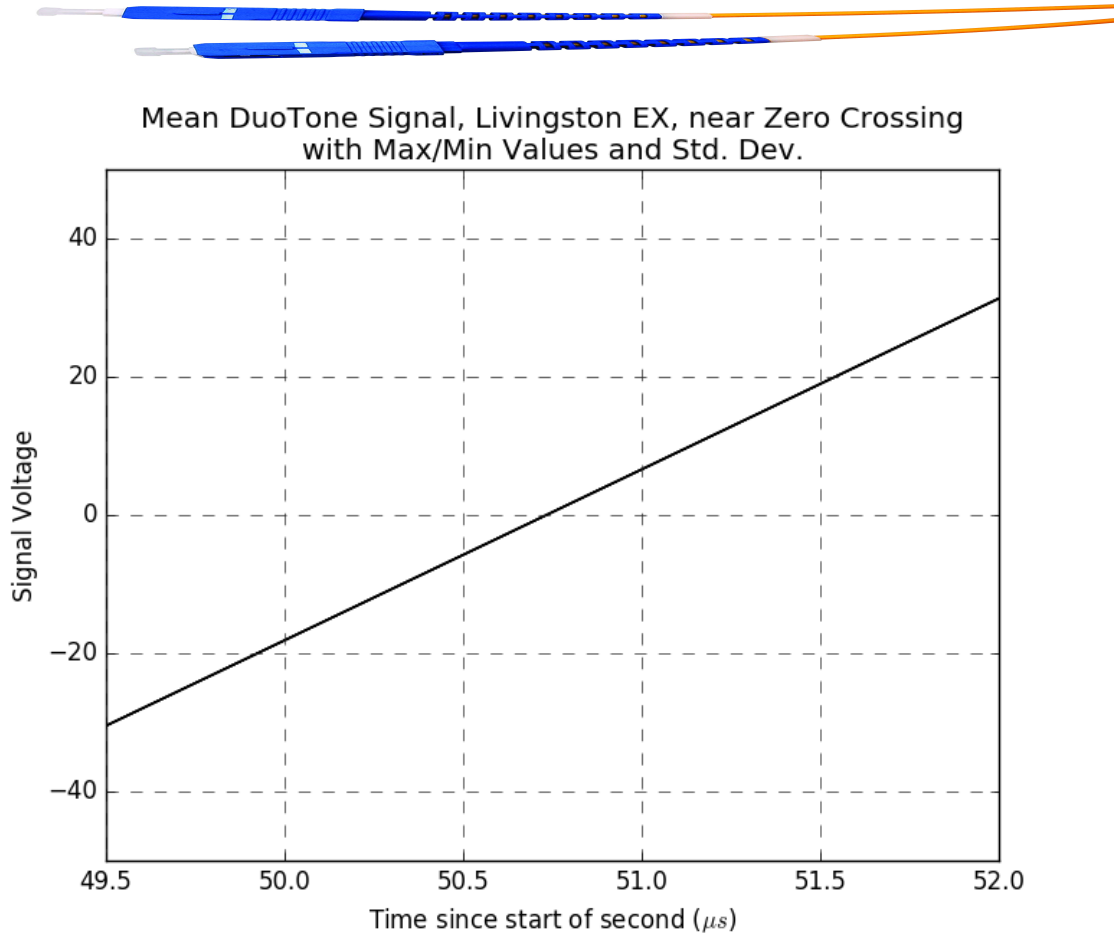


Figure 9: Zero crossing region of the second-to-second average of the DuoTone witness signals around the second edge at Livingston EX for the hour surrounding the GW170104 event candidate. Open circle reflect the average signal, the green error bars indicate the standard deviation, and the ends of the fine black error bars show the maximum/minimum for each data point. Please note that the green error bar is so small that it is still covered by the circular symbol. The line through the data points guide the eye to help visualize the zero crossing which is best visible on this magnification setting and is at $\sim 50.7\mu\text{s}$, out of which $50.25\mu\text{s} = 6.70\mu\text{s}$ (DuoTone generation delay) + $43.55\mu\text{s}$ (decimation filter delay) is accounted for.

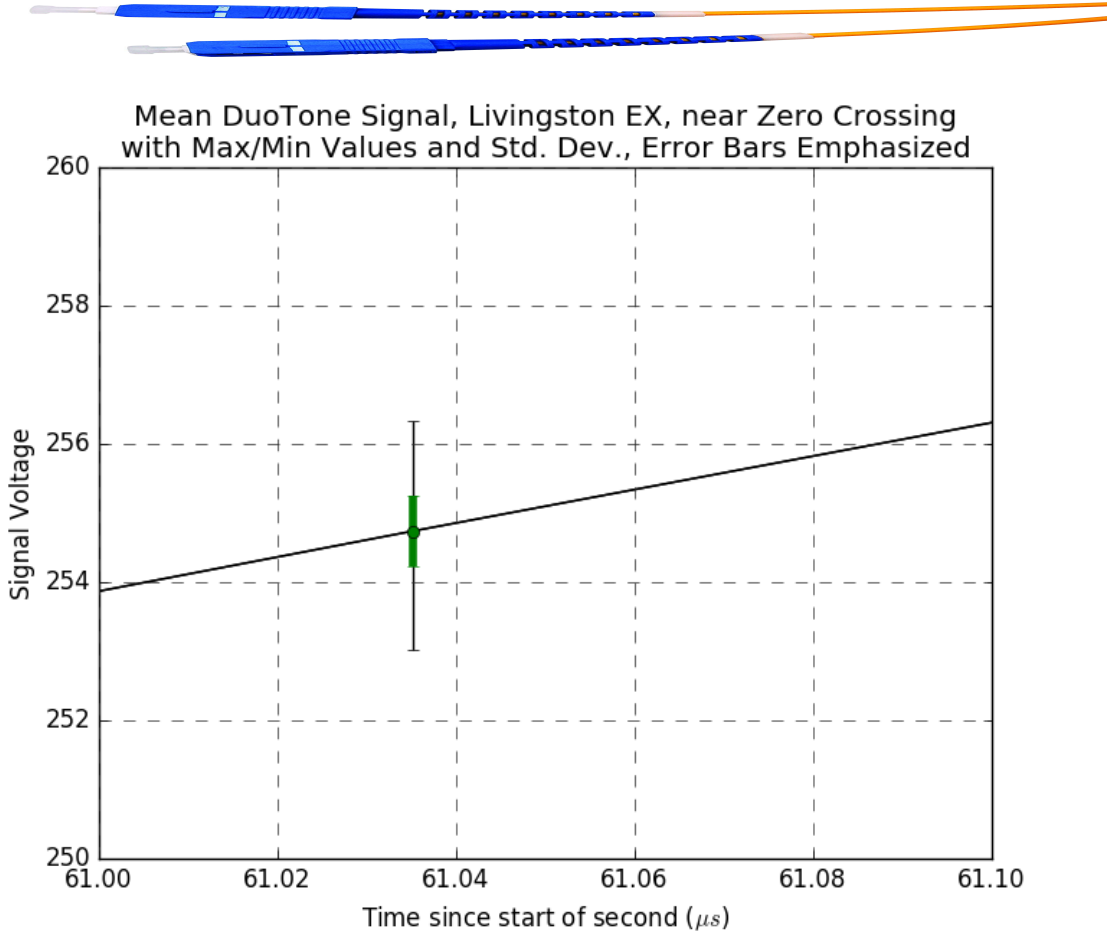


Figure 10: Zero crossing region of the second-to-second average of the DuoTone witness signals around the second edge at Livingston EX for the hour surrounding the GW170104 event candidate. The open circle reflect the average signal, the green error bar indicates the standard deviation, and the ends of the fine black error bar shows the maximum/minimum for the data point. The size of the green error bar indicates very small error on the zero crossing.



4. IRIG-B Signal Decoding

The IRIG-B signal from independent GPS clocks was digitized and recorded at each site in order to provide an independent cross-check for the aLIGO Timing System's absolute timestamp. These signals were decoded (as specified in [Timing IRIG-B Signal Decoding Test, T1500391](#)) and plotted for the time of the candidate event GW170104, observed at 1167559936= Wed Jan 04 10:11:58 UTC 2017. The time code was found to be in agreement with the timestamp of the datastream (note that Hanford's IRIG-B signals are in GPS time; the 18 second difference with UTC is due to leap seconds). Figures 11 through 14 below show the externally generated IRIG-B signals at Hanford and Livingston along with their decoded times. They are consistent with the aLIGO Timing System's timestamp as used by the aLIGO framewriting computers.



Figure 11

One Second of IRIG-B Signal at LHO X End Station
Decoded GPS Time: Wed Jan 04 10:12:16 2017
Actual Time: Wed Jan 04 10:11:58 UTC 2017

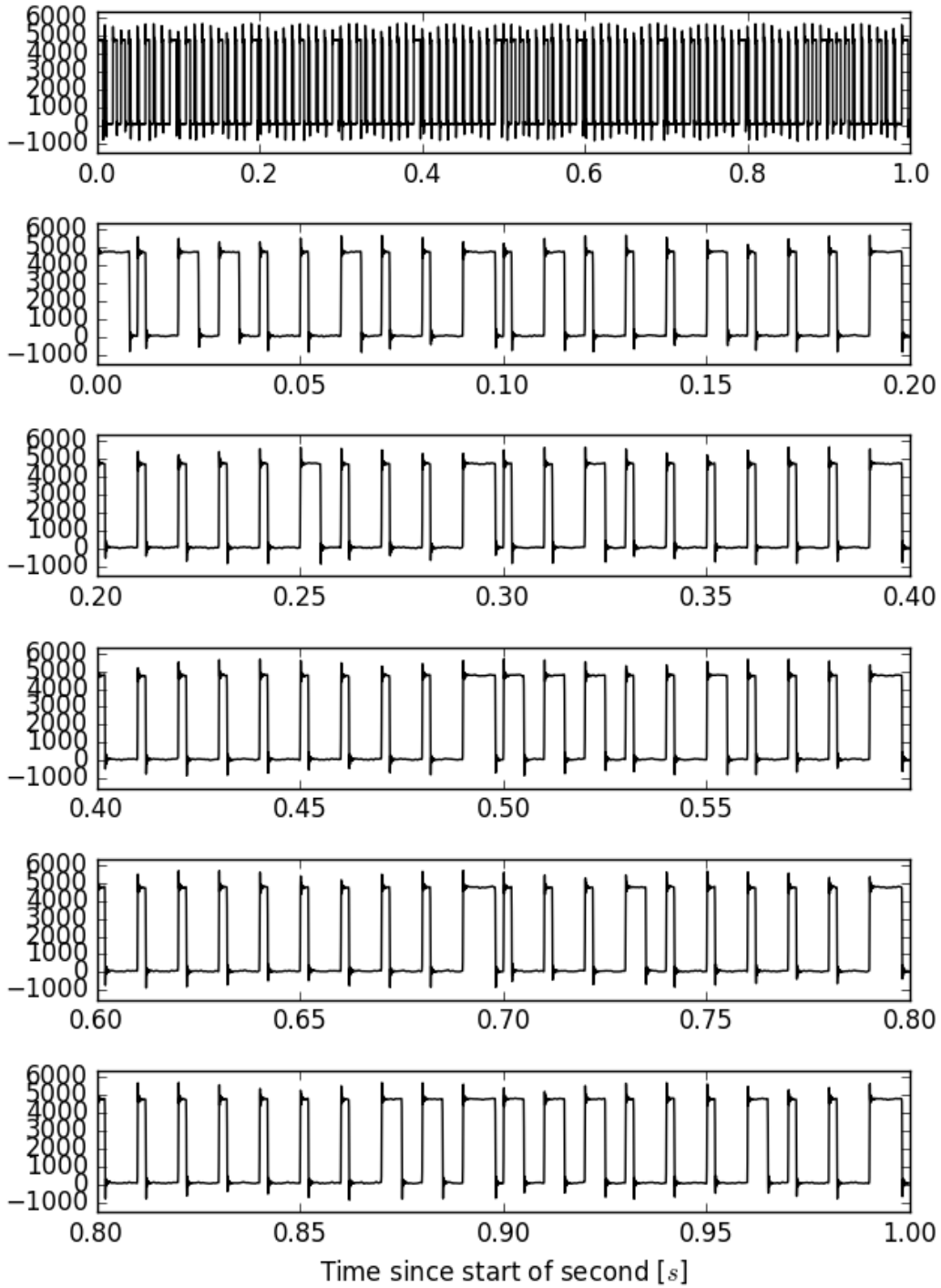




Figure 12

One Second of IRIG-B Signal at LHO Y End Station
Decoded Time: Wed Jan 04 10:12:16 2017
Actual Time: Wed Jan 04 10:11:58 UTC 2017

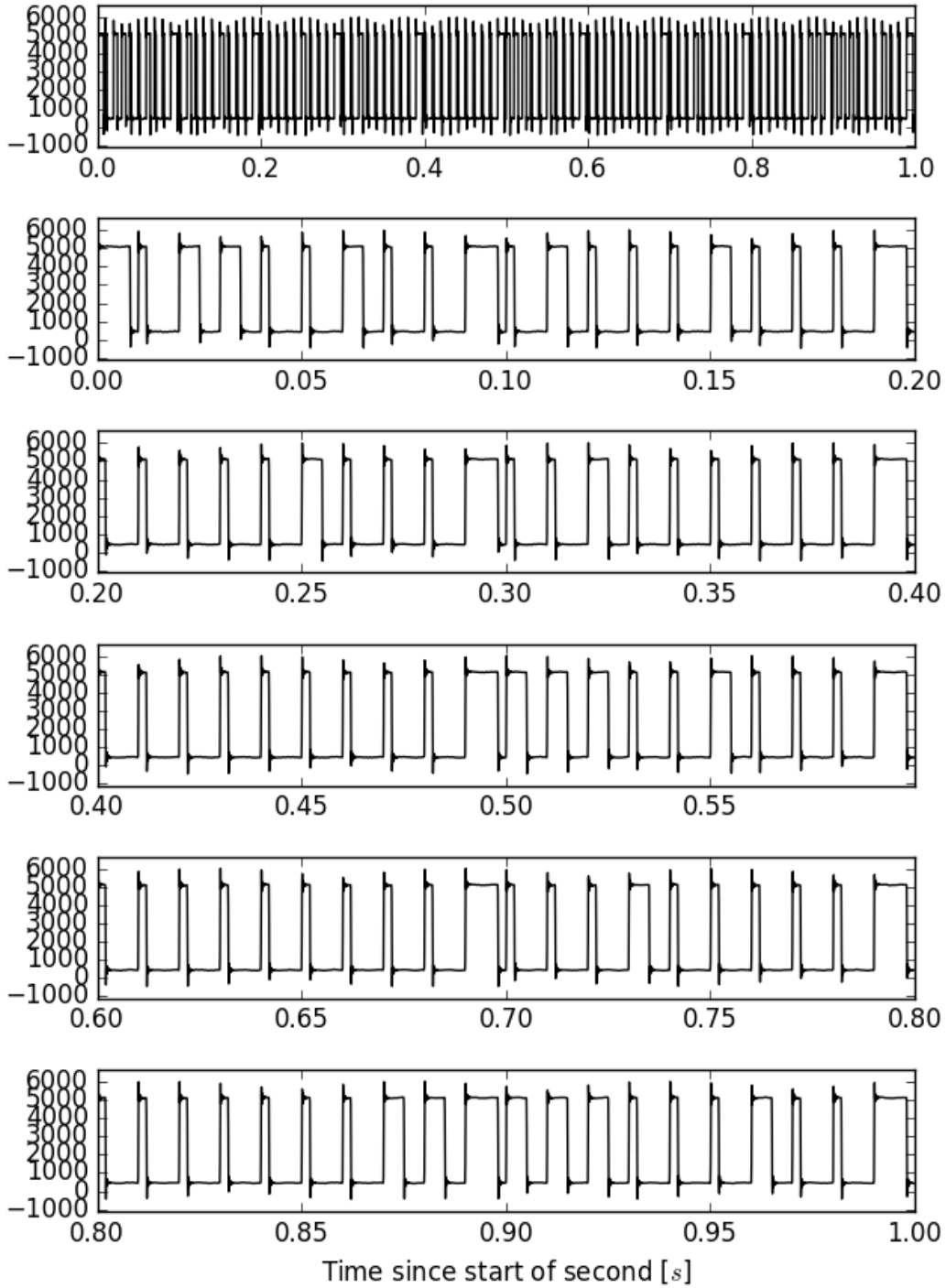




Figure 13

One Second of IRIG-B Signal at LLO X End Station
Decoded GPS Time: Wed Jan 04 10:11:58 2017
Actual GPS Time: Wed Jan 04 10:11:58 UTC 2017

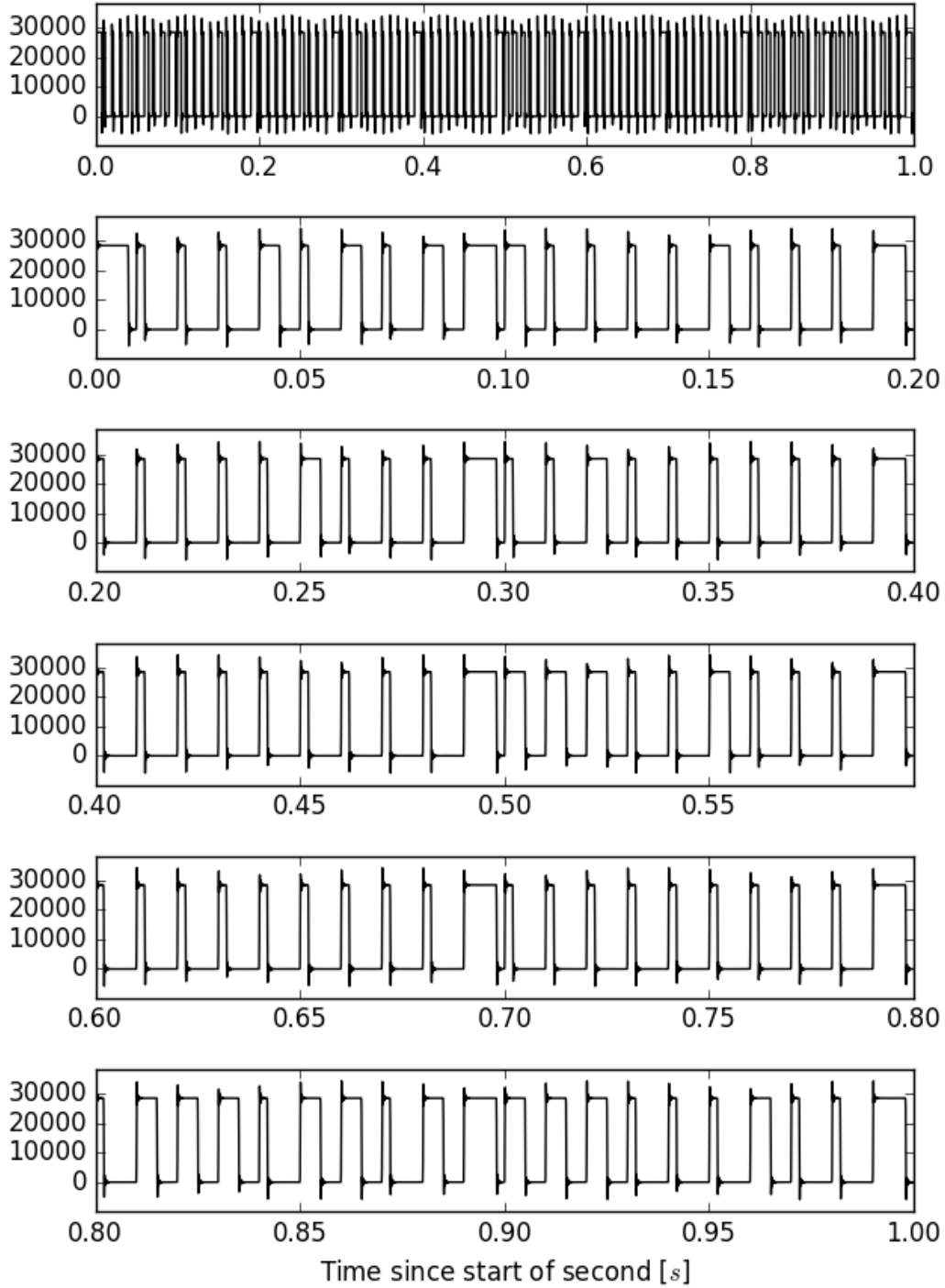
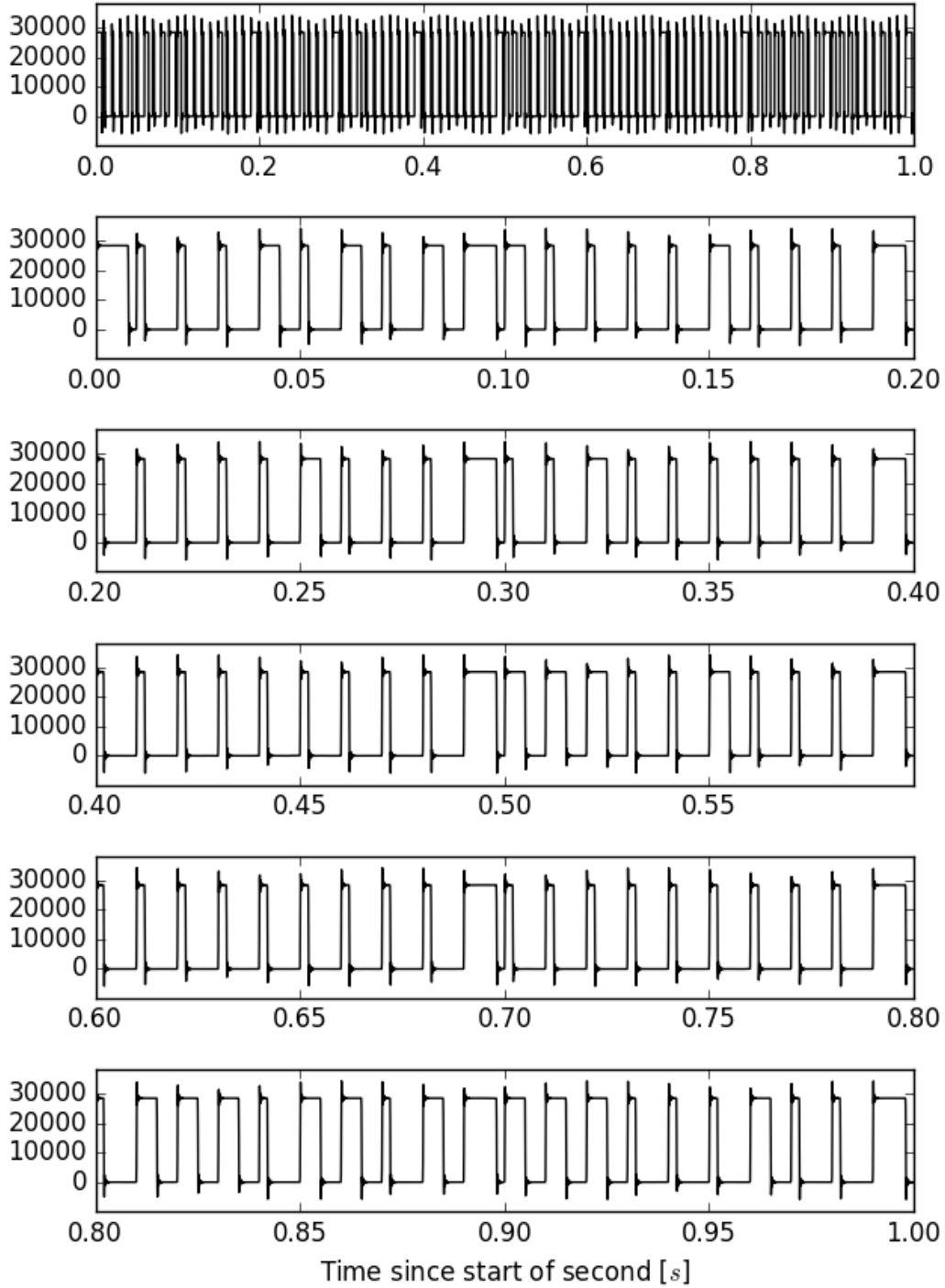




Figure 14

One Second of IRIG-B Signal at LLO Y End Station
Decoded Time: Wed Jan 04 10:11:58 2017
Actual Time: Wed Jan 04 10:11:58 UTC 2017





5. Conclusion

All the sanity checks shown in this document indicate that the timing performance of the aLIGO detectors around the candidate event GW170104, observed at 1167559936= Sat Wed Jan 04 10:11:58 UTC 2017 is according to specifications.